

AD-A075 207

AEROSPACE CORP EL SEGUNDO CA SPACE SCIENCES LAB

F/G 4/1

CORRELATED OBSERVATIONS OF AURORAL ARCS, ELECTRONS, AND X-RAYS --ETC(U)

SEP 79 P F MIZERA, W A KOLASINSKI, J B BLAKE

F04701-78-C-0079

UNCLASSIFIED

TR-0079(4960-05)-2

SAMSO-TR-79-53

NL

| OF |

AD
A075207



END
DATE
FILMED
11-79

DDC

LEVEL *12*

12

AD A075207

Correlated Observations of Auroral Arcs, Electrons, and X-Rays from a DMSP Satellite

P. F. MIZERA, J. G. LUHMANN,
W. A. KOLASINSKI, and J. B. BLAKE
→ Space Sciences Laboratory
Laboratory Operations
The Aerospace Corporation
El Segundo, Calif. 90245

28 September 1979

DDC
RECEIVED
OCT 19 1979
E

Interim Report

APPROVED FOR PUBLIC RELEASE;
DISTRIBUTION UNLIMITED

DDC FILE COPY

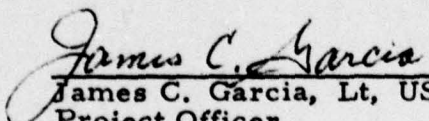
Prepared for
SPACE AND MISSILE SYSTEMS ORGANIZATION
AIR FORCE SYSTEMS COMMAND
Los Angeles Air Force Station
P.O. Box 92000, Worldway Postal Center
Los Angeles, Calif. 90009

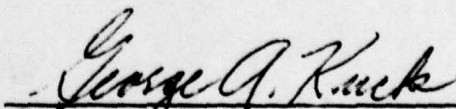
20 10 18 019

This interim report was submitted by The Aerospace Corporation, El Segundo, CA 90245, under Contract No. F04701-78-C-0079 with the Space and Missile Systems Organization, Deputy for Technology, P. O. Box 92960, Worldway Postal Center, Los Angeles, CA 90009. It was reviewed and approved for The Aerospace Corporation by G. A. Paulikas, Director, Space Sciences Laboratory. Lieutenant J. C. Garcia, SAMSO/DYXT, was the project officer for Technology.

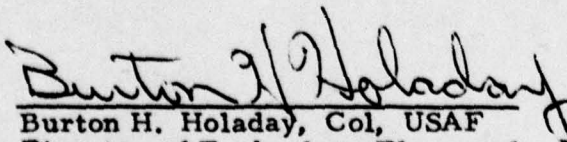
This report has been reviewed by the Information Office (OI) and is releasable to the National Technical Information Service (NTIS). At NTIS, it will be available to the general public, including foreign nations.

This technical report has been reviewed and is approved for publication. Publication of this report does not constitute Air Force approval of the report's findings or conclusions. It is published only for the exchange and stimulation of ideas.


James C. Garcia, Lt, USAF
Project Officer


George A. Kuck, Maj, USAF, Chief
Technology Plans Division

FOR THE COMMANDER


Burton H. Holaday, Col, USAF
Director of Technology Plans and
Analysis
Deputy for Technology

UNCLASSIFIED

SECURITY CLASSIFICATION OF THIS PAGE (When Data Entered)

19 REPORT DOCUMENTATION PAGE		READ INSTRUCTIONS BEFORE COMPLETING FORM
1. REPORT NUMBER 18 SAMSO TR-79-53	2. GOVT ACCESSION NO.	3. RECIPIENT'S CATALOG NUMBER
4. TITLE (and Subtitle) 6 CORRELATED OBSERVATIONS OF AURORAL ARCS, ELECTRONS, AND X-RAYS FROM A DMSP SATELLITE.	5. TYPE OF REPORT & PERIOD COVERED 9 Interim rept.	
7. AUTHOR(s) 10 Paul F./Mizera, Janet G./Luhmann, Wojciech A./Kolasinski, J. Bernard/Blake	6. PERFORMING ORG. REPORT NUMBER 14 TR-0079(4960-05)-2	
9. PERFORMING ORGANIZATION NAME AND ADDRESS The Aerospace Corporation El Segundo, Calif. 90245	8. CONTRACT OR GRANT NUMBER(s) 15 F04701-78-C-0079	
11. CONTROLLING OFFICE NAME AND ADDRESS Space and Missile Systems Organization Air Force Systems Command Los Angeles, Calif. 90009	10. PROGRAM ELEMENT, PROJECT, TASK AREA & WORK UNIT NUMBERS	
14. MONITORING AGENCY NAME & ADDRESS (if different from Controlling Office) 12 22	12. REPORT DATE 11 28 September 1979	
	13. NUMBER OF PAGES 21	
	15. SECURITY CLASS. (of this report) Unclassified	
	15a. DECLASSIFICATION/DOWNGRADING SCHEDULE	
16. DISTRIBUTION STATEMENT (of this Report) Approved for public release; distribution unlimited.		
17. DISTRIBUTION STATEMENT (of the abstract entered in Block 20, if different from Report)		
18. SUPPLEMENTARY NOTES		
19. KEY WORDS (Continue on reverse side if necessary and identify by block number) Aurorae Bremsstrahlung Remote Sensing Precipitating Electrons Auroral X-Rays		
20. ABSTRACT (Continue on reverse side if necessary and identify by block number) The first simultaneous observations, made from a single DMSP satellite, of visible auroral arcs, precipitating primary electrons, and atmospheric bremsstrahlung x-rays are presented for a moderately disturbed auroral event. Measured electron fluxes were used to compute absolute x-ray distributions expected at the satellite altitude. The agreement between the calculated and measured x-ray spectra is sufficiently good to suggest that global auroral energy input can be monitored by an orbiting x-ray spectrometer.		

DD FORM 1473
(FACSIMILE)

UNCLASSIFIED

SECURITY CLASSIFICATION OF THIS PAGE (When Data Entered)

407512 Lhu

PREFACE

The successful on-orbit performance of the x-ray instrument was due to the work of many people. Major M. Schneider, Captain J. Cunningham and J. Shrum had major roles in the development of the instrument and the integration aboard the DMSP satellite. Engineering, construction and testing work was ably carried out by N. Katz, C. King, D. Katsuda, S. Imamoto, W. Wong, and G. Roberts. Data processing was performed by G. Boyd and G. Pihos. The authors also would like to acknowledge the assistance of Dr. D. McKenzie concerning the proportional counter calibration and Capt. M. Holcomb, USAF-AWS, for supplying the auroral optical data. One of us (J. G. L.) would like to thank Prof. A. Liuzzi at the University of Lowell for providing unpublished laboratory data pertaining to aluminum bremsstrahlung measurements.

Accession For		<input checked="checked" type="checkbox"/>
NTIS GRA&I		
DDC TAB		
Unannounced		
Justification		
By _____		
Distribution/		
Availability Codes		
Dist	Avail and/or	
	special	

A

CONTENTS

PREFACE	1
INTRODUCTION	5
INSTRUMENTATION	7
RESULTS	9
ANALYSIS	15
SUMMARY AND DISCUSSION	17
REFERENCE	19

FIGURES

1. DMSP-F2 Aurorae, X-Rays, and Electrons, October 19, 1977. (a) Midnight and evening auroral arcs in the wavelength band between 475 to 750 nm recorded by the DMSP visible scanner. (b) Energy-time spectrogram of upcoming Bremsstrahlung x-rays and downgoing electrons as a function of time along the satellite ground track (Fig. 1a) 10
2. Open Circles Represent the Differential Number Flux of Precipitating Electrons Associated with the Five Arc Systems Identified in Fig. 1a 12
3. Absolute X-Ray Differential Number Fluxes Associated with the Five Arc Systems (Fig. 1a) 14

PRECEDING PAGE BLANK

INTRODUCTION

The technique of measuring auroral particle fluxes directly with instruments carried by orbiting satellites is inherently plagued with severe limitations. Only particles near the satellite are detected and hence small data samples from extremely limited regions of space are obtained. Furthermore, time gaps equal to the orbital period are present in these limited data samples, rendering them of little use in observing the temporal evolution of auroral forms.

While a network of satellites could provide extensive spatial coverage of the auroral regions, a more practical alternative would be provided by a remote sensing technique which, in principle, could indirectly measure representative energy spectra of precipitating particles away from the location of the satellite. Visible auroral scanners flown on the DMSP and Isis satellites represented a major step in that direction. However, only semi-qualitative estimates of the total precipitating electron population could be inferred, even when direct electron measurements were made on the same satellite (Mizera et al., 1975; Meng, 1976; Liu et al., 1977).

Precipitating auroral electrons generate bremsstrahlung which is related in a well-understood way to the primary electron fluxes and spectra (Berger and Seltzer, 1972; Luhmann and Blake, 1977). Therefore, x-ray measurements by satellites provide an attractive means of obtaining true global coverage of particle precipitation phenomena. Imhof and his coworkers, in the first of an extensive list of papers on satellite x-ray measurements (Imhof et al., 1974; Imhof, 1975; Imhof et al., 1975a; 1975b) have pointed out potential applications of this technique. However, their x-ray measurements were at energies above 50 keV and therefore outside the 1-10 keV energy range of primary interest in auroral electron precipitation studies. Correlations between auroral electrons and x-rays with energy above ≈ 2 keV have been obtained by means of rocket probes fired into individual arcs (Wilson et al., 1969) but these data are of extremely limited spatial and temporal extent.

In this paper some initial results of auroral bremsstrahlung measurements, obtained with instrumentation on the second Block 5D DMSP satellite, are presented at

energies above approximately 1.5 keV. Unlike studies of this type reported previously, this investigation correlates x-ray data directly with both simultaneous observations of precipitating electron fluxes in the 0.05 eV - 20 keV energy range and with optical images of the associated auroral forms obtained by sensors on the same satellite.

Several examples of electron spectra associated with individual optical arcs have been used to predict the bremsstrahlung intensity emitted from the region of each arc. Good agreement in both the spectral form and absolute magnitude is obtained between the calculated and measured x-ray spectra for a number of cases. The analysis suggests that the inverse procedure of deducing reasonably accurate values of precipitating electron fluxes from measurements of auroral bremsstrahlung is also possible.

INSTRUMENTATION

The data for this study were obtained by instruments on the second (F2) DMSP satellite of the Block 5D series (1977-044A). The satellite is in an approximately circular orbit of 830 km altitude with a 99° inclination. The orbital plane of the three-axis stabilized satellite is located near the dawn-dusk meridian. The three instruments of interest onboard the F2 satellite are an x-ray spectrometer, an electron spectrometer, and an optical imaging system.

The x-ray instrument uses a proportional counter and an array of four cadmium telluride detectors as the sensing elements. The proportional counter covers the energy range from 1.4 keV to ≥ 20 keV and the cadmium telluride sensor has an energy range from 15 keV to ≥ 90 keV. The proportional counter uses an equal mixture of Ar and Xe with 10% CO_2 as a quench gas and has a 2 mil beryllium entrance window. A series of aluminum slits provide collimation for the proportional counter and define a rectangular field-of-view whose center is directed towards the nadir. The half-intensity points of the field-of-view are $\pm 2^{\circ}$ along the satellite track and $\pm 14^{\circ}$ crosstrack. The proportional counter uses pulse-shape discrimination circuitry to distinguish between signals due to soft x-rays, and other ionizing events such as charged particles which leave a long ionization track in the counter. Use of this circuitry reduces the proportional counter background to locally-generated soft bremsstrahlung. Counts due to penetrating charged particles, hard x-rays, and gamma rays are negligible. Fifteen energy channels from 1.4 keV to ≈ 20 keV are used, with a channel separation comparable to the proportional counter resolution. The low-energy cutoff is determined by the transmission of the beryllium entrance window, and the (effective) high-energy limit by the transparency of the counter gas to x-rays above a few tens of keV. Six other energy channels are used which are either ungated or in anticoincidence with the x-ray signal from the pulse-shape discrimination circuitry; these channels serve as background and performance monitors. The absolute efficiency of the proportional counter was measured in the laboratory for x-ray energies between 1.3 keV and 20 keV.

The four cadmium telluride semiconductor detectors are embedded in an anticoincidence shield against penetrating charged particles and mounted on the spacecraft such that the outward-pointing symmetry axis of the cadmium telluride-scintillator configuration is directed toward the nadir. Each detector normally makes an angle of 30° with the scintillator axis, and the detectors are placed symmetrically at 90° intervals in the azimuthal direction. This arrangement, along with the satellite motion, provides a coarse direction-finding capability. Each cadmium telluride detector has five energy channels. Four of these channels are operated in anticoincidence with the scintillation counter and count events with energy deposits in the cadmium telluride detector above thresholds of 15, 30, 60 and 90 keV; the fifth channel counts all events above a 15 keV threshold without the anticoincidence criterion. An additional data channel monitors the singles rate in the scintillator.

Precipitating electrons are measured with a pair of cylindrical electrostatic analyzers (ESAs) which use channeltron detectors. The lower-energy electrostatic analyzer covers the energy range from 50 eV to 1 keV, and the higher-energy electrostatic analyzer from 1 keV to 20 keV. Each ESA has eight energy channels sampled sequentially for 0.1 second. Thus, a complete 16-point spectrum is acquired once per second. These electrostatic analyzers are mounted on the DMSP satellite with the apertures directed toward the zenith. The instrument is described in detail in reports by Pantazis et al. (1977) and Huber et al. (1977).

The auroral photographs were obtained from the Block 5D "visible" imaging system which has a passband from approximately 475 nm to 750 nm (FWHM) (E. Rogers, private communication, 1978). It should be noted that this passband differs significantly from the "visible" passband of the earlier Block 5B/C satellites of approximately 590 nm to 1010 nm (FWHM) (Rogers et al., 1974).

RESULTS

Auroral data taken on October 19, 1977 near 0130 hrs. UT over the north polar region are summarized in Figs. 1a and 1b. Figure 1a shows the visible arcs recorded by the primary sensor on the DMSP-F2 satellite. For the arcs shown in Fig. 1a, the familiar green and red lines of oxygen at 5577\AA and 6300\AA contribute relatively more than for previous DMSP auroral images whose wavelength response extended beyond $10\,000\text{\AA}$. The narrow auroral arcs shown in Fig. 1a are located between invariant latitudes of 63° and 71° near 20 hrs magnetic local time. The scale and alignment of the auroral photograph have been chosen to match the time scale at the bottom of the spectrogram in Fig. 1b. The center line drawn in Fig. 1a is the projection of the satellite orbit down to the auroral arcs. The outer parallel lines in Fig. 1a represent the cross-track field-of-view of the x-ray sensor. The cross-track dimension is approximately 375 km. Typically, the width of the arcs crossed by the satellite is approximately 0.2° latitude or 20-25 km. This dimension is approximately one half of the in-track field-of-view. In Fig. 1a, local midnight is toward the top and local evening is toward the right hand side, in the region of the structured auroral arcs.

Figure 1b shows an energy-time spectrogram of the precipitating electrons and x-rays produced by the bremsstrahlung process. Electron fluxes with energies from ≈ 0.05 to 1 keV are displayed on the bottom panel; data for electrons with energies from ≈ 1 to 20 keV are given on the middle panel and data for x-rays with energies from ≈ 1.5 to 18 keV are shown in the top panel. The electron instrument is pointed toward the zenith; the x-ray sensor is pointed toward the nadir. The gray scales on the right of Fig. 1b are in units of differential energy flux for the precipitating electrons and in arbitrary units (proportional to the differential number flux) for the x-rays. Universal time, invariant latitude and magnetic local time are noted at the bottom of Fig. 1b every 100 sec. As the satellite crossed the evening auroral arcs going equatorward from the polar cap the electron spectrometer recorded a number of discrete enhancements. These individual structures can be associated with the auroral arcs in Fig. 1a almost on a one to one basis. We have classified the individual optical structures in universal time, viz., 5373, 5393,

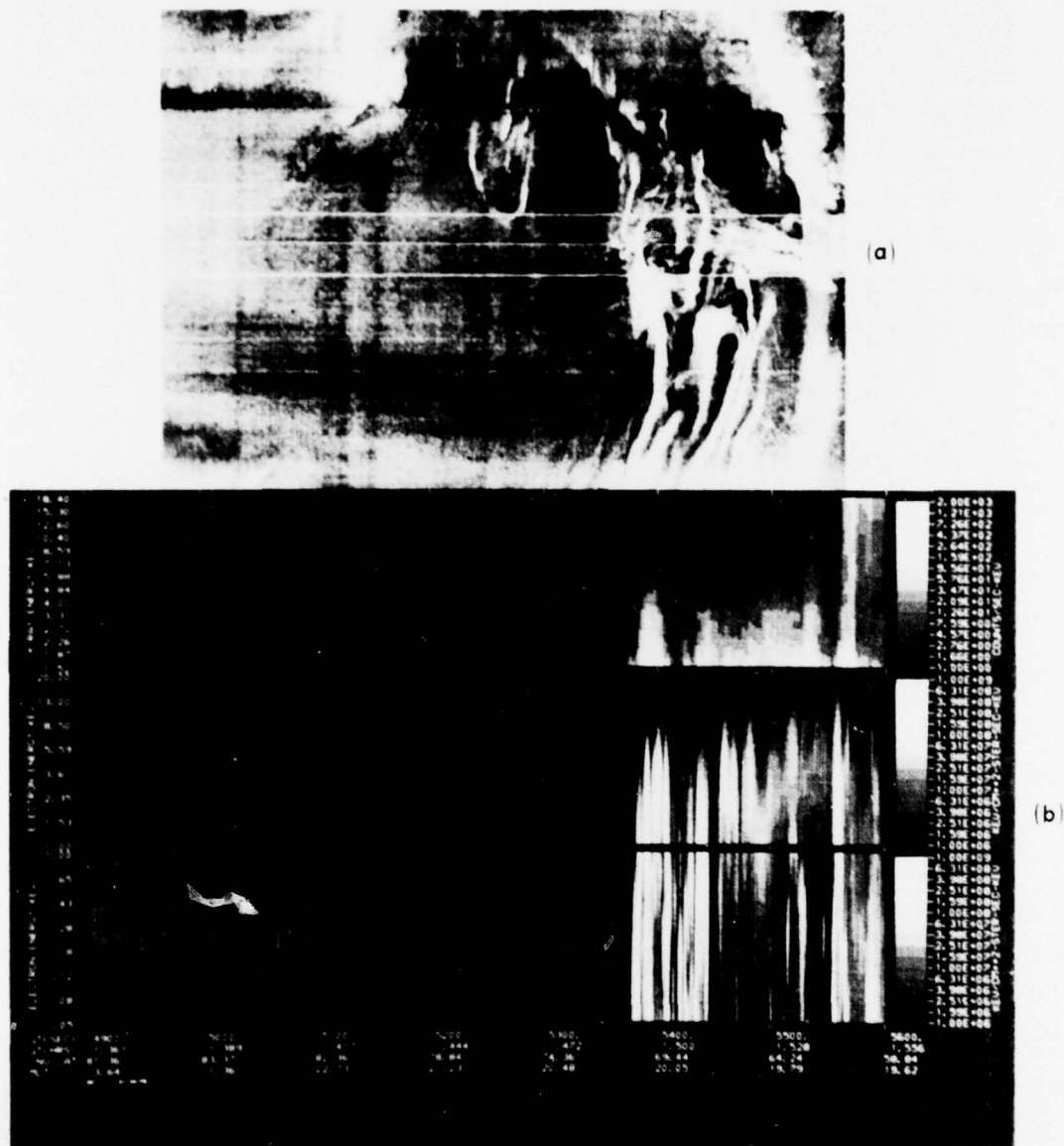


Fig. 1. DMSP-F2 Aurorae, X-Rays, and Electrons, October 19, 1977.
 (a) Midnight and evening auroral arcs in the wavelength band between 475 to 750 nm recorded by the DMSP visible scanner.
 (b) Energy-time spectrogram of upcoming Bremsstrahlung x-rays and downgoing electrons as a function of time along the satellite ground track (Fig. 1a).

5425, 5446, and 5538 sec UT. These examples are hereafter designated as cases #1 through #5. In order to compare the electron fluxes directly with the auroral arcs, one must consider the geometry of the magnetic field. At altitudes around 830 km, the time difference between the nadir crossing of the foot of a magnetic field line and the field line at satellite altitude is approximately 17 sec. One must shift the electron fluxes in Fig. 1b by this amount. Moreover, the nadir intersection depicted in Fig. 1a as the satellite ground track is separated in longitude from the foot of the field line at any given time by approximately 1° . At these latitudes, this separation corresponds to approximately 50 km. Therefore, the electron fluxes shown in Fig. 1b would enter the atmosphere west (toward noon) of the satellite ground track by approximately 10% of the projected x-ray field-of-view.

The preponderance of the emitted visible light results from auroral arcs in the pre-midnight sector. Fig. 1b shows individual electron structures, peaked at energies of a few keV, as the satellite crosses the arcs. These weak inverted 'V' structures are reasonably well correlated with individual auroral arcs when the time lag, discussed previously, is included.

Enhancements in the x-ray flux occur at times coincident with the auroral arcs seen in Fig. 1b. Whenever the satellite encounters fluxes of intense energetic electrons, the latter produce local bremsstrahlung in the field-of-view of the x-ray sensor. Cases #1 through #5 were chosen at times when local electron fluxes were low enough to produce negligible effects in the measured x-ray intensity from the earth. For the five cases presented here, the electron fluxes were averaged over a time comparable to the crossing of each individual arc. Figure 2 shows the electron spectrum obtained for each example.

The electron fluxes associated with the five arcs in Fig. 1a display peaked energy spectra commonly associated with inverted 'V' structures (Ackerson and Frank, 1972; Evans, 1974; Mizera et al., 1976). The inverted 'V' signature has been associated with an electric field acceleration (Gurnett, 1972; Swift et al., 1976; Mizera and Fennell, 1977). In all five cases considered here, the electron input spectrum showed peaks in the few keV energy range. This feature associated with quiet discrete auroral arcs, has been discussed recently by Meng (1977) and by Arnoldy and Lewis (1977).

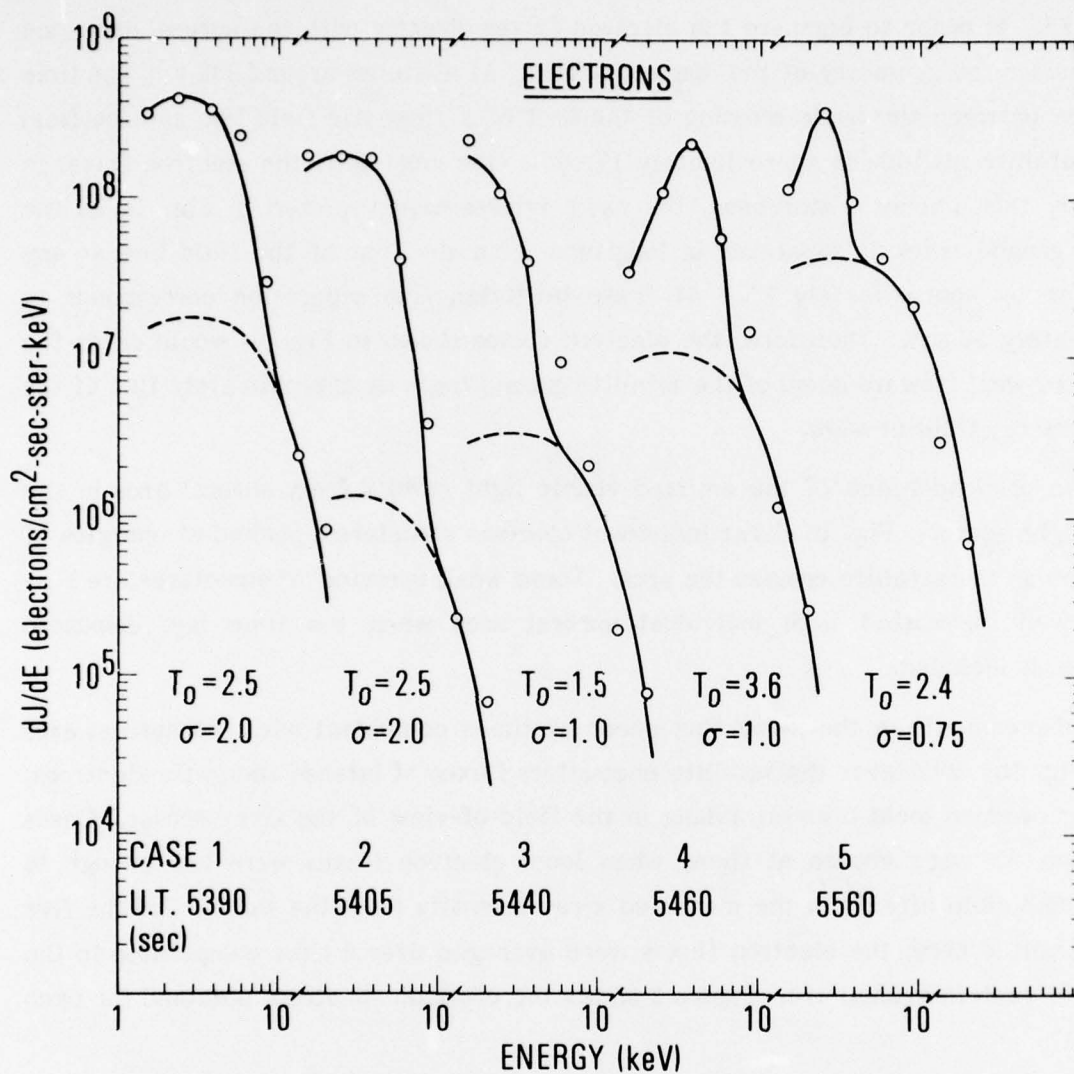


**Fig. 2. Open Circles Represent the Differential Number Flux of Pre-
cipitating Electrons Associated with the Five Arc Systems
Identified in Fig. 1a.**

X-ray spectra were derived from time averages taken when the satellite nadir crossed (or nearly crossed) the arcs shown in Fig. 1a. Absolute fluxes of the x-rays were calculated using the following assumptions. The geometric factor was obtained using the standard response of uniform flux impinging on a rectangular collimator. This procedure assumes that the entire field-of-view of the x-ray sensor is uniformly illuminated by the source of x-rays. Since the visible auroral arcs did not fill the entire field-of-view, a grid was placed over the photograph and the fraction of illumination was estimated. This is a gross approximation to the true instrument response; nevertheless, the absolute x-ray fluxes shown in Fig. 3 are in remarkable agreement with the predicted values up to approximately 8 keV. The counting rates in the higher energy channels were at background level.

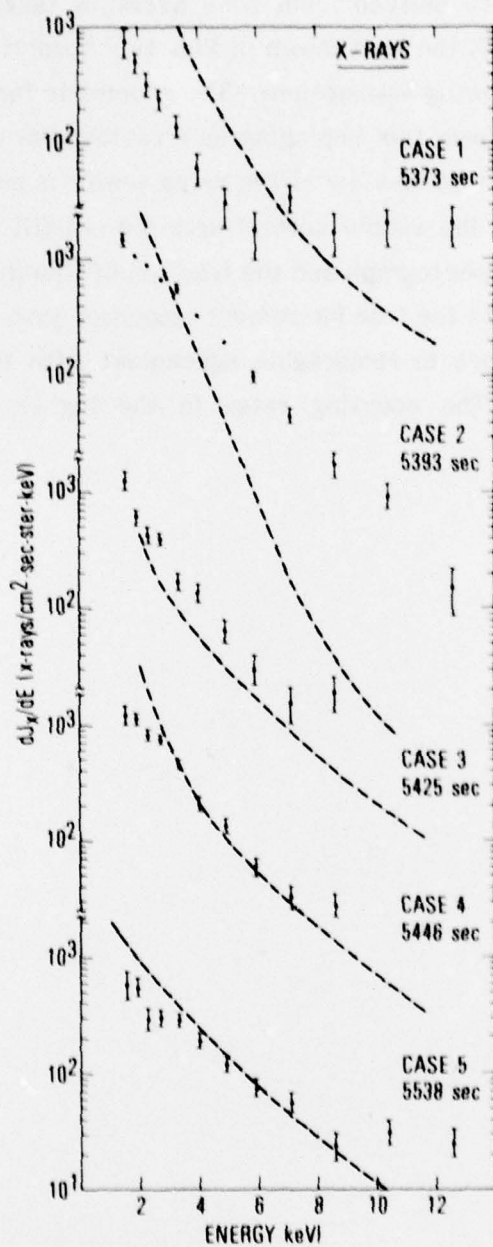


Fig. 3. Absolute X-Ray Differential Number Fluxes Associated with the Five Arc Systems (Fig. 1a)

ANALYSIS

It was pointed out in the introduction that x-ray measurements are a better alternative for large-scale studies of auroral zone energy deposition than electron measurements. The latter give information about the precipitating electrons only on magnetic field lines crossed by the satellite, while x-rays can provide information about any part of the auroral oval within the detector's field of view. However, the inference of energy deposition from x-ray measurements requires a reliable method of deriving the unobserved electron spectrum from the observed x-ray spectrum.

As discussed in the preceding section, the precipitating electron spectra observed at the DMSP altitude in connection with x-ray arcs are generally of the inverted 'V' type (see Fig. 1b). Evans (1974) and others have found that the energy spectra associated with inverted 'V' structures resemble Maxwell-Boltzmann distributions which have been accelerated by a DC potential drop. The functional form that describes an accelerated thermal distribution is given by:

$$J(E) \propto E \exp \left[- (E - V_0) / E_0 \right] \quad (1)$$

where E is the electron energy, E_0 is the temperature in units of energy, and V_0 is the DC potential that varies across the latitude extent of the inverted 'V' structure.

Figure 2 shows the electron spectra at 5390, 5405, 5440, 5460, and 5560 seconds UT in Fig. 1b. These were selected to represent the five previously identified optical arcs designated as cases #1 through #5. The electron spectra are not well described by the simple functional form of (1); however, the data have been averaged over the entire core of complex inverted 'V' structures which include a range of potential drops. This averaging procedure is appropriate for the correlation of electrons and x-rays discussed here, since the field-of-view of the x-ray instrument encompasses broad optical forms which, when mapped along field lines to the satellite orbit, span a length corresponding

to the entire width of an observed inverted 'V' structure. It is found that the averaged spectra can be approximated by a Gaussian of central energy T_0 and halfwidth σ plus a Maxwellian with a temperature $E_0 = 3$ keV. Figure 2 shows the Gaussian parameters used in each of the five cases; the dashed curves show the contributions of the Maxwellian component.

The ability to interpret auroral bremsstrahlung data in terms of primary electron input is demonstrated by comparing x-ray spectra calculated from the electron fluxes shown in Figure 2 with the observed x-ray spectra. The identification of the x-rays correlated with each of the five arcs was described in the preceding section, and illustrated in Fig. 1. The calculated x-ray spectrum for each of the five electron spectra was obtained using a method described elsewhere (Luhmann, 1977; Luhmann and Blake, 1977). The absolute x-ray flux between 1 and 15 keV is computed under the assumptions that 1) the observed averaged electron spectrum describes the precipitating electrons that generate the observed x-rays, 2) characteristic line emission (Oxygen K_{α} at .525 keV, Nitrogen K_{α} at .396 keV and Argon K_{α} at 2.96 keV) does not contribute to the observed flux, 3) the observed x-rays consist of photons that travel to the detector at angles within 14° of the nadir, and 4) the emitting atmosphere uniformly fills the 14° acceptance angle. The latter restrictions are required because the calculation was initially designed to give the omnidirectional bremsstrahlung flux from a uniformly emitting plane-parallel atmosphere. The 14° angle represents the half-width at half-maximum of the cross-track detector field of view. Division of the calculated flux by the solid angle corresponding to 14° provides a measure of the unidirectional flux entering the detector aperture.

Absolute bremsstrahlung intensities predicted by the calculations are shown in Figure 3 together with the measured x-ray fluxes. Three of the five cases (#3, #4, and #5) show excellent absolute agreement between the calculated and experimental spectra. The two cases (#1 and #2), for which the agreement is not good, correspond to situations for which the ground track of the satellite did not intersect the brightest part of the arc in the field of view of the x-ray sensor (see Figure 1a). Thus it is not surprising that for cases #1 and #2, the electron spectra shown in Fig. 2 fail to represent the average electron spectrum responsible for most of the x-ray flux detected by the sensor as it is crossed the aurora near 5400 sec UT.

SUMMARY AND DISCUSSION

In general, a degree of ambiguity exists in the deduction of a primary electron spectrum from a bremsstrahlung spectrum. A specific functional form must be assumed for the electron distribution. Peaked electron spectra, such as those shown in Fig. 2 are associated with quiet-time auroral arcs. In this study the electron spectra corresponding to the five auroral arcs in Fig. 1a were adequately described by the combination of a Gaussian and a Maxwellian form. Figure 3 shows the x-ray spectra calculated from these empirical fits, compared with the observed x-ray spectra between 1.5 and 8 keV. In three out of the five cases, the measured electron spectral form leads to an accurate prediction of the absolute x-ray spectrum. The poor agreement in the two remaining cases can be attributed to the fact that the measured electron spectrum did not represent the brightest auroral form in the field-of-view of the x-ray detector.

The foregoing analysis suggests that it is possible to determine electron spectra associated with auroral arcs by means of x-ray measurements. The procedure for inferring the spatial distribution of energy deposition in the atmosphere then consists of two steps. Following the results of the present analysis, it is assumed that all auroral electron spectra, associated with discrete arcs, are represented by Gaussian functions with the central energy T_0 and width σ as parameters plus a Maxwellian with an adjustable amplitude and a temperature of 3 keV. The predicted x-ray spectra for various values of T_0 and σ can be examined to determine which values produce the best fit to the x-ray data. In the final step, the electron spectra inferred in this manner can be used to calculate the local auroral energy desposition by well established methods (Rees, 1963; Berger and Seltzer, 1972; Luhmann, 1977).

REFERENCES

Ackerson, K. L. and L. A. Frank, Correlated Satellite Measurements of Low-Energy Electron Precipitation and Ground-Based Observations of a Visible Auroral Arc, J. Geophys. Res., 77, 1972.

Arnoldy, R. L. and P. B. Lewis, Jr., Correlation of Ground-Based and Topside Photometric Observations with Auroral Electron Spectra Measurements at Rocket Altitudes, J. Geophys. Res., 82, 5563, 1977.

Berger, M. J. and Seltzer, S. M., Bremsstrahlung in the Atmosphere, J. Atmos. Terr. Phys., 34, 85, 1972.

Evans, D. S., Precipitating Electron Fluxes formed by a Magnetic Field Aligned Potential Differences, J. Geophys. Res., 79, 2853, 1974.

Gurnett, D. A., Electric Field and Plasma Observations in the Magnetosphere, Critical Problems of Magnetospheric Physics, ed. by E. R. Dyer, Nat. Acad. Sci., Wash., D. C., 123, 1972.

Huber, A., P. Pantazis, A. L. Besse and P. L. Rothwell, Calibration of the SSJ/3 Sensor on the DMSP Satellites, AFGL-TR-77-0202, Nat. Tech. Info. Cen., 1977.

Imhof, W. L., G. H. Nakano, R. G. Johnson, and J. B. Reagan, Satellite Observations of Bremsstrahlung from Widespread Energetic Electron Precipitation Events, J. Geophys. Res., 79, 565, 1974.

Imhof, W. L., Review of Rocket and Satellite Measurements of X-Rays from Electron Precipitation at High Latitudes, Proc. International Conference on X-Rays in Space, University of Calgary, Calgary, Alberta, Canada, 741, 1975.

Imhof, W. L., G. H. Nakano, E. E. Gaines, and J. B. Reagan, A Coordinated Two-Satellite Study of Energetic Electron Precipitation Events, J. Geophys. Res. 80, 3629, 1975a.

Imhof, W. L., G. H. Nakano, and J. B. Reagan, Satellite Observations of X-rays Associated with Energetic Electron Precipitation Near the Trapping Boundary, J. Geophys. Res. 80, 3629, 1975b.

Liu, A.T.R., D. Venkatesan, C. D. Anger, S.-I. Akasofu, W. J. Heikkila, J. D. Winningham and J. R. Burrows, Simultaneous Observations of Particle Precipitations and Auroral Emissions by the ISIS 2 Satellite in the 19-24 MLT Sector, J. Geophys. Res., 82, 2210, 1977.

Luhmann, J. G., "Auroral Bremsstrahlung Spectra in the Atmosphere", J. Atmos. Terr. Phys., 38, 595, 1977.

Luhmann, J. G. and J. B. Blake, "Calculations of Soft Auroral Bremsstrahlung and K_{α} Line Emission at Satellite Altitude", J. Atmos. Terr. Phys., 39, 913, 1977.

Meng, C.-I., Simultaneous Observations of Low-Energy Electron Precipitation and Optical Auroral Arcs in the Evening Sector by the DMSP-32 Satellite, J. Geophys. Res., 81, 1976.

Meng, C.-I., Precipitation Characteristics of Quiet Auroral Arcs, EOS, Trans. Am. Geophys. Union, 58, 1209, 1977.

Mizera, P. F., D. R. Croley, Jr., F. A. Morse, and A. L. Vampola, Electron Fluxes and Correlations with Quiet Time Auroral Arcs, J. Geophys. Res., 80, 2129, 1975.

Mizera, P. F., D. R. Croley, Jr., and J. F. Fennell, Electron Pitch-Angle Distributions in an Inverted 'V' Structure, Geophys. Res. Letters, 3, 149, 1976.

Mizera, P. F. and J. F. Fennell, Signatures of Electric Fields from High and Low Altitude Particle Distributions, Geophys. Res. Letters, 4, 311, 1977.

Pantazis, J., A. Huber and M. P. Hagan, Design of Electrostatic Analyzer AFGL-TR-77-0120, Nat. Tech. Info. Cen., 1977.

Rees, M. H., Auroral Ionization and Excitation by Incident Energetic Electrons, Planet. Space Sci., 11, 1209, 1963.

Rogers, E. H., D. F. Nelson, and R. C. Savage, Auroral Photography from a Satellite, Science, 183, 951, 1974.

Swift, D. W., H. C. Stenback-Nielsen and T. J. Hallinan, An Equipotential Model for Auroral Arcs, J. Geophys. Res. 81, 3931, 1976.

Wilson, B. G., A. J. Baxter and D. W. Green, Low Energy Bremsstrahlung X-ray Spectra from a Stable Auroral Arc, Can. J. Phys. 47, 2427, 1969.

LABORATORY OPERATIONS

The Laboratory Operations of The Aerospace Corporation is conducting experimental and theoretical investigations necessary for the evaluation and application of scientific advances to new military concepts and systems. Versatility and flexibility have been developed to a high degree by the laboratory personnel in dealing with the many problems encountered in the nation's rapidly developing space and missile systems. Expertise in the latest scientific developments is vital to the accomplishment of tasks related to these problems. The laboratories that contribute to this research are:

Aerophysics Laboratory: Launch and reentry aerodynamics, heat transfer, reentry physics, chemical kinetics, structural mechanics, flight dynamics, atmospheric pollution, and high-power gas lasers.

Chemistry and Physics Laboratory: Atmospheric reactions and atmospheric optics, chemical reactions in polluted atmospheres, chemical reactions of excited species in rocket plumes, chemical thermodynamics, plasma and laser-induced reactions, laser chemistry, propulsion chemistry, space vacuum and radiation effects on materials, lubrication and surface phenomena, photo-sensitive materials and sensors, high precision laser ranging, and the application of physics and chemistry to problems of law enforcement and biomedicine.

Electronics Research Laboratory: Electromagnetic theory, devices, and propagation phenomena, including plasma electromagnetics; quantum electronics, lasers, and electro-optics; communication sciences, applied electronics, semiconducting, superconducting, and crystal device physics, optical and acoustical imaging; atmospheric pollution; millimeter wave and far-infrared technology.

Materials Sciences Laboratory: Development of new materials; metal matrix composites and new forms of carbon; test and evaluation of graphite and ceramics in reentry; spacecraft materials and electronic components in nuclear weapons environment; application of fracture mechanics to stress corrosion and fatigue-induced fractures in structural metals.

Space Sciences Laboratory: Atmospheric and ionospheric physics, radiation from the atmosphere, density and composition of the atmosphere, aurorae and airglow; magnetospheric physics, cosmic rays, generation and propagation of plasma waves in the magnetosphere; solar physics, studies of solar magnetic fields; space astronomy, x-ray astronomy; the effects of nuclear explosions, magnetic storms, and solar activity on the earth's atmosphere, ionosphere, and magnetosphere; the effects of optical, electromagnetic, and particulate radiations in space on space systems.

THE AEROSPACE CORPORATION
El Segundo, California